EPJ Web of Conferences **193**, 02003 (2018) https://doi.org/10.1051/epjconf/201819302003
*FISSION 2017*

# Total kinetic energy and fragment mass distributions from fission of Th-232 and U-233

*Daniel* Higgins[1,2*], *Uwe* Greife[1], *Shea* Mosby[2], and *Fredrik* Tovesson[2]

[1]Colorado School of Mines, Physics Department, 1500 Illinois Ave, Golden, Colorado, USA
[2]Los Alamos National Laboratory, PO Box 1663, Los Alamos, New Mexico, USA

**Abstract.** Properties of fission in Th-232 and U-233 were studied at the Los Alamos Neutron Science Center at incident neutron energies from sub-thermal to 40 MeV. Fission fragments are observed in coincidence using a twin ionization chamber with Frisch grids. The average total kinetic energy released from fission and fragment mass distributions are calculated from observations of energy deposited and conservation of mass and momentum. Accurate experimental measurements of these parameters are necessary to better understand the fission process in isotopes relevant to the thorium fuel cycle, in which Th-232 is used as a fertile material to generate the fissile isotope of U-233. This process mirrors the uranium breeder process used to produce Pu-239 with several potential advantages including the comparative greater abundance of thorium, inherent nuclear weapons proliferation resistance, and reduced actinide production. Thus, there is increased interest in the thorium fuel cycle to meet future energy demands and improve safety and security while increasing profitability for the nuclear power industry. This research is ongoing and preliminary results are presented.

## 1 Introduction

A significant amount of energy is released in nuclear fission and the majority of that energy is in the form of kinetic energy of the fission fragments formed after scission. The average total kinetic energy (TKE) released by neutron-induced fission of actinides is approximately 180 MeV on average and is well represented by a normal distribution with a typical full width at half maximum of approximately 25 MeV [1-3]. The average value of this TKE distribution has been shown by previous experiments to have a dependence on incident neutron energy and although it has been well measured at thermal energy, this dependency has not been well characterized at higher incident neutron energies [4]. In this experiment, properties of fission in Th-232 and U-233 are studied at the Los Alamos Neutron Science Center (LANSCE) at neutron energies from thermal to 40 MeV. Fission fragments are observed in coincidence using a twin ionization chamber with Frisch grids. The average total kinetic energy released from fission and fragment mass distributions are calculated from observations of energy deposited and conservation of mass and momentum. Accurate experimental measurements of these parameters are necessary to better understand the fission process in isotopes relevant to the Th fuel cycle, in which Th-232 is used as a fertile material to generate the fissile isotope

* Corresponding author: dhiggins@mines.edu

U-233. This process mirrors the uranium breeder process used to produce Pu-239 with several potential advantages including the comparatively greater abundance of Th, inherent nuclear weapons proliferation resistance, and reduced actinide production [5]. For these reasons, there is increased interest in the Th fuel cycle to meet future energy demands and improve safety and security while increasing profitability for the nuclear power industry.

## 2 Experiment

### 2.1 Facility

This experiment is conducted at LANSCE, a linear accelerator at the Los Alamos National Laboratory (LANL) capable of producing up to 800 MeV protons. Two facilities were used to take measurements, the Weapons Neutron Research (WNR) facility and the Lujan Neutron Scattering Center. At WNR the high energy proton beam is directed onto an unmoderated tungsten spallation source which generates neutrons from 200 keV to approximately 600 MeV. Both the Th-232 and U-233 targets are measured in the 90L WNR flight path. Fission in U-233 from thermal neutrons is measured at the Lujan Center where protons are delivered to the 1L Target area which uses a water moderator and a liquid hydrogen moderator to slow neutrons down to thermal and sub-thermal energies.

### 2.2 Experimental set up

This experiment is conducted using a steel bodied cylindrical ionization chamber with two back to back detection volumes positioned on axis along the neutron beamline. Each volume has a circular anode with a Frisch grid and a shared cathode between the two. The cathode also supports the sample target material which is positioned at the center of the cathode normal to the beamline. There are two samples used in this experiment, one contains the fertile isotope Th-232 and the other contains the fissile isotope U-233. Both samples are supported on a thin $100 \pm 10$ μg/cm$^2$ carbon foil backing which is itself secured to the cathode by a thin aluminum ring. The Th sample consists of a full circle deposit of 603.6 μg of isotopically pure Th-232 with 192.1 μg/cm$^2$ area density. The U-233 sample enriched to >99% is also a full circle deposit that contains 226.1 μg of U at an area density of 72 μg/cm$^2$. Constant current density molecular plating was used to create this sample [6]. The plating solvent used in this process, an isopropanol-isobutanol mixture, has been shown to result in a residual layer of cracked solvent molecules on the surface of the target referred to as crud [7]. Energy loss of fission fragments travel through the solvent layer, backing and target material itself is corrected. The ionization chamber uses P-10 fill gas (90% Ar, 10% CH4); the anodes are biased at 1000 V and the cathode at -1500 V.

### 2.3 Data acquisition

The accelerator delivers a pulse signal when the proton beam reaches the spallation target which serves as the start signal for the neutron time of flight. The signal from the cathode is used as the stop time for the neutron time of flight. The two anode signals are used to determine the energy of the ionizing particle in the gas and the two signals from the Frisch grids to determine the angle of emission of the particle.

# 3 Method

## 3.1 Neutron energy

The neutron energy is calculated by using relativistic kinetic energy and applying the neutron time of flight method. For data collected from the Th-232 sample, a few apparent features can be identified in the uncalibrated time of flight spectrum. A small sharp peak around 80 ns is caused by gamma induced fission from photons released from the spallation target, the photofission peak and is useful for calibrating the neutron time of flight spectrum since the photons that caused these events have a known speed.

A sharp change in counts around 380 ns is associated with a sudden rise in the Th-232 fission cross section which is the result of second chance fission. The time difference between the photofission peak and the onset of second chance fission is used to calculate the flight path length based on kinetic energy. This process is repeated based on two other smaller features in the uncalibrated time of flight spectrum located near 685 ns and 710 ns which were correlated with sharp features in the Th-232 cross section for fission at 1.58 and 1.7 MeV respectively. The flight path length is taken as the average of the three resultant length calculations, all of which are within 5 mm of each other, and is found to be 11.885 m. Using this length measurement the time of flight spectrum can be calibrated based on the position of the photofission peak which is then converted to neutron energy as shown in Fig. 1.

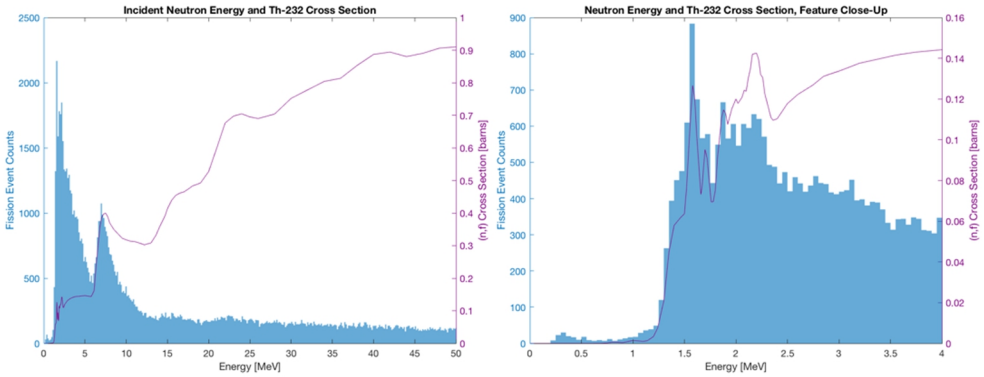


**Fig. 1.** On the left, the neutron energy spectrum, shown in blue, is compared to the neutron induced fission cross section, shown in purple, for Th-232. On the right a close up view at lower energy shows a good correlation between features in both the neutron energy spectrum and the cross section.

There is an overall trend in increasing events measured at lower neutron energy due to the increased flux of neutrons at lower energy levels. The rise in the cross section associated with second chance fission at 6 MeV is seen to correspond with a rise in fission events. A close up view of this spectrum reveals that smaller features in the cross section, such as those between 1 and 3 MeV also correspond well with features in the neutron energy spectrum.

A separate method was used to calculate the flight path length for the data collected with the U-233 sample installed. A small block of carbon, approximately 3 cm by 3 cm by 5 cm, was placed in the path of the neutron beam upstream from the detector. There is a sharp feature in the neutron scattering cross section for carbon at 2.078 MeV which prevents a large percentage of neutrons at that energy from reaching the detector. The carbon notch and the photofission peak in the neutron time of flight spectrum for U-233 can be used in the same manner as were the fission cross section features for Th-232 to calculate the flight path length. This length was found to be 11.883 m which differs from the Th-232 length measurement by

less than 3 mm. The strong agreement between the calculated flight path lengths using the two methods indicates that this calculation was performed correctly and therefore all events have a reliable measurement of the incident neutron energy.

### 3.2 Fragment energy

Determining the energy of the fission fragments is done by analyzing the anode pulse heights as well as calculating angle of emission from the grid signals. The anode pulse heights from the two volumes show a bimodal distribution with a narrow feature at higher energy and a broader feature at lower energy. The narrow feature is generated by the light fragment since it will carry away a greater the share of kinetic energy [8].

The anode pulse heights for the two volumes are not exactly aligned, the difference between the two is due to differences between the detector volumes. The first is that before the fragments enter the volume they pass through both the target sample material and the backing while in the other volume fragments only pass through the target. Therefore, fragments passing through the backing will lose much more energy than those that do not. The next difference is due to the difference between the laboratory reference frame and the center of mass frame. The incident neutron carries with it an appreciable amount of momentum which then drives the energy distribution into its direction of motion in the laboratory reference frame resulting in an increased deposition of energy in the downstream volume of the detector. This can be corrected for by converting to the center of mass reference frame based on the energy of the incident neutron and conservation of momentum. Another difference between the volumes which must be corrected for is that the gains on the preamps through which the signals pass and are amplified are very close to one another, however, they are not exactly the same. This is corrected for by a linear calibration of one volume to the other by applying two Gaussian fits to the two features, for both light and heavy fragments, for the anode pulse height distributions of each volume. Once these corrections have been calculated and applied, the anode pulse height distributions of the two volumes should overlap one another, as shown in Fig. 2, and it becomes possible to calibrate the anode pulse height to energy. The two features in the anode spectra are fit to Gaussian distributions, the means of which are taken as the light and heavy fragments from which a linear fit can be made to calibrate for energy.

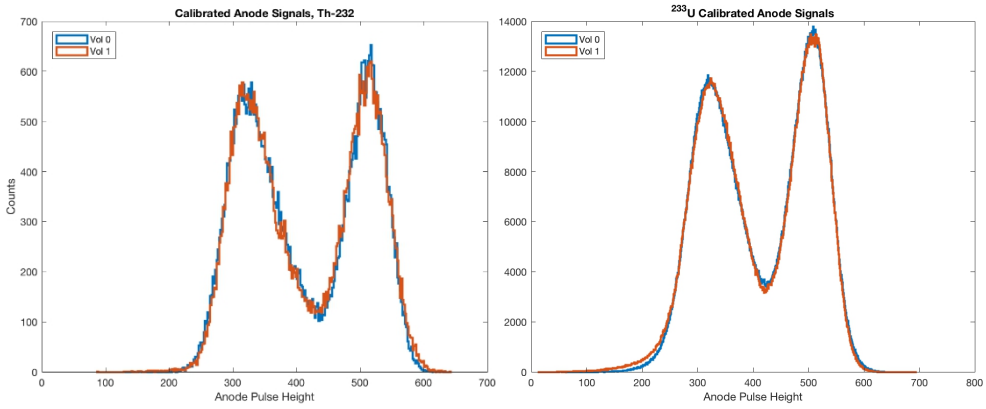


**Fig. 2.** The anode pulse height spectra for both detector volumes from the Th-232 data (left) and U-233 (right) corrected for all differences between volumes. The spectra lie directly on top of each other which indicates that the correction factors have been appropriately applied.

### 3.3 Neutron emission

The mass and energy of the fission fragments is found using a calculation based on conservation of mass and momentum that iteratively adjusts the masses and corrects for mass dependent variations such as the pulse height defect until the mass of the fission fragments converge to within a threshold [9]. It is dependent on having the correct mass of the system, both before and after scission. The mass of the combined nucleus is based on the mass of the target nucleus plus the mass of the incident neutron. However, this value can vary with energy of the incident neutron due to the onset of second and higher chance fission reactions [10]. The probability of these reactions increases with increasing incident neutron energy which is reflected in the cross section for multi-chance fission as shown for U-233 in Fig. 3. The mean mass of the combined nucleus depends directly on the relative probability of various multi-chance fission reactions and so varies continuously across incident neutron energies.

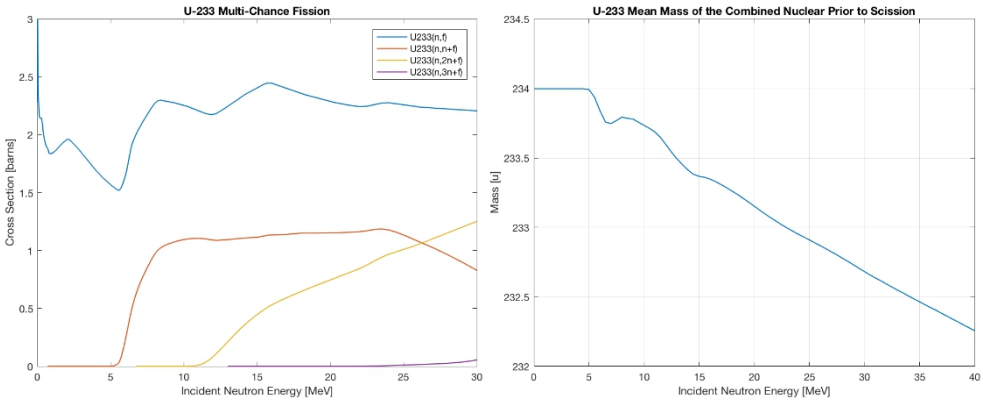


**Fig. 3.** Cross sections for first, second, third, and fourth chance fission in U-233 shown on the left. The proportional probability of various fission chances varies continuously which is used in this work to determine the mean mass of the combined nucleus, shown on the right.

The 2E analysis method used for this experiment also requires the mass after scission which is the mass of the fission fragments. Fragments emit a small number of neutrons almost immediately after scission which reduces their mass. There is a dearth of experimental data for this parameter for Th-232 and U-233, so this value is found using the General Observables in Fission (GEF) model [11]. Each iteration of the 2E analysis results in a new estimate for the mass of the fission fragment and therefore the neutron emission, which is mass dependent, and must be determined for each iteration. It is not practical to run the GEF code for each iteration, so it is run beforehand over the full range of incident neutron energies and a surface plot is interpolated across all masses and energies. Then, when the iterative analysis is performed, it references this neutron emission surface. By doing this, the GEF code can be run with large enhancement factors for improved counting statistics.

### 3.4 Deliverables

The 2E analysis iteratively recalculates the fragment masses and energies based on the anode signal calibrated to energy, the pulse height defect, the neutron emission, and the mean mass of the combined nucleus. This iteration is performed until the new calculated mass differs from the previously calculated mass by less than some threshold depending on the mass resolution of the detector. The output values include the mass and energy of both the light and heavy fission fragments as well as the energy of the incident neutron. The energy of the

two fragments is taken as the total kinetic energy released from fission. When events are grouped together by incident neutron energy, the total kinetic energies are expected to form a normal distribution, the mean of which is the average total kinetic energy for that incident neutron energy. In this way a plot is made which shows the trend of average total kinetic energy as it varies across the range of incident neutron energies. This trend for both Th-232 and U-233 will be one of the two final deliverables of this work which can be compared to past experiments in the low energy range. The other value of interest calculated in this experiment is the mass of the fission fragments. The mass distribution can then be examined to see how it changes across different incident neutron energies and compared to past experiments. This research is ongoing and final results are still forthcoming.

## References

1. M.B. Chadwick et al. Nucl. Data Sheets **112**, 2887 (2011)
2. J.W. Meadows, C. Budtz-Jørgensen. ANL/NDM-64, Argonne National Lab. (1982)
3. V. Viola, K. Kwiatkowski, M. Walker. Phys. Rev. C **31**, 1550 (1985)
4. D.G. Madland. Nucl. Phys. A **772**, 113 (2006)
5. *Thorium Fuel Cycle – Potential Benefits and Challenges*, IAEA-TECDOC-1450 (2005)
6. World Nuclear Association, world-nuclear.org (2016)
7. W. Loveland. J. Radioanal. Nucl. Ch. **307**, 1591 (2016)
8. A. Vascon, N. Wiehl, T. Reich, J. Drebert, K. Eberhardt, Ch.E. Düllmann. Nucl. Instr. Meth. A **721**, 35 (2013)
9. L. Meitner, O.R. Frisch. Nature **143**, 239 (1939)
10. F. Vivès. *Mesure des Propriétés des Fragments de Fission de la Réaction $^{238}$U(n,f) à des Énergies de Neutrons Incidents Jusqu'à 5.8 MeV*. Université Bordeaux I (1998)
11. H. Naik, Sadhana Mukherji, S. Suryanarayana, K. Jagadeesan, S. Thakare, S. Sharma. Nucl. Phys. A **952**, 100 (2016)
12. K.H. Schmidt, B. Jurado, C. Amouroux. *General Description of Fission Observables: GEF Model*. NEA-OECD, NEA/DB/DOC2014-1 (2014)